The Hydration Enthalpies of Md^{3+} and Lr^{3+}

W. BRÜCHLE, M. SCHÄDEL

Gesellschaft für Schwerionenforschung mbH, D-6100 Darmstadt, F.R.G.

U. W. SCHERER*, J. V. KRATZ**

Institut für Kernchemie, Universität Mainz, D-6500 Mainz, F.R.G.

K. E. GREGORICH, D. LEE, M. NURMIA, R. M. CHASTELER, H. L. HALL, R. A. HENDERSON and D. C. HOFFMAN

Lawrence Berkeley Laboratory, University of California, Berkeley, Calif. 94720, U.S.A.

(Received October 26, 1987)

Abstract

Lawrencium (3-min ^{260}Lr) and lighter actinides were produced in the bombardment of a ^{249}Bk target with ^{18}O ions and loaded onto a cation exchange column in 0.05 M α-hydroxyisobutyrate solution at pH = 4.85, together with the radioactive lanthanide tracers ^{166}Ho, ^{171}Er and ^{171}Tm. In elutions with 0.12 M α-hydroxyisobutyrate solution (pH = 4.85), trivalent Lr was eluted exactly together with the Er tracer and Md was eluted close to Ho. Lr elutes much later than expected based on the known elution positions of the lighter actinides and the expected analogy to the elution positions of the homologous lanthanides. From the measured elution positions, ionic radii were calculated for Lr^{3+} and Md^{3+}. Semi-empirical models allow the calculation of the heat of hydration from the ionic radii, resulting in $\Delta H_{hyd} \cong -3654$ kJ/mol for Md^{3+} and $\Delta H_{hyd} \cong -3685$ kJ/mol for Lr^{3+}.

Introduction

Studies of the chemical properties of the heaviest actinides and comparison with the properties of the lanthanides are of particular interest because they help assess the influence of relativistic effects [1]. These cause a stabilization of the s- and p-orbitals in the actinides. By analogy with lutetium, the last member of the lanthanide series, which has an electronic structure of $[Xe]4f^{14}5d^{1}6s^{2}$, the structure of lawrencium would be expected to be $[Rn]5f^{14}6d^{1}7s^{2}$. However, because of relativistic effects, Brewer [1] predicted the configuration would be $[Rn]5f^{14}7s^{2}7p^{1}$ and Dirac–Fock calculations [2] confirm this prediction. The relativistic stabilization and contraction of the radially symmetric s- and p-orbitals leads to a secondary effect: the axially symmetric orbitals (e.g. 5f) expand because the nuclear charge is shielded more effectively. For the heaviest actinide ions this might result in ionic radii different from non-relativistic extrapolations. These changes should also be reflected in some thermodynamical properties, such as the heat of formation.

Because elements above fermium must be produced in accelerators and are available as short-lived isotopes only in quantities of a few atoms at a time, such bulk quantities cannot be measured directly. Therefore, Keller [3] has suggested breaking the heat of formation down with the aid of the Born–Haber cycle (Fig. 1) into its component parts. heat of sublimation, ionization energy and heat of hydration. In principle, the heat of sublimation could be determined by gas chromatography. The ionization potential needs to be calculated [2] or could perhaps be determined by laser excitation. The heat of hydration can be derived with the help of semi-empirical equations [4–6] from the ionic radius.

To determine the ionic radius of Lr^{3+} (and that of Md^{3+}), and thus their heats of hydration, we used a chromatographic method as proposed by Marcus and Kertes [7]: ionic radii of aquo ions of the same charge and coordination number undergoing the same type of chemical process are correlated linearly to the

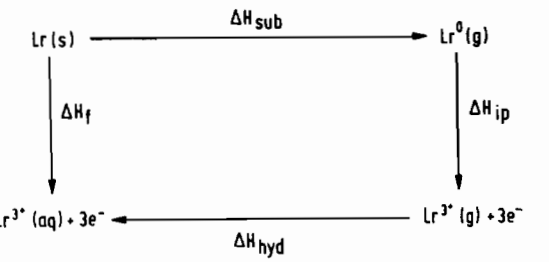

Fig. 1. Born–Haber cycle for the heat of formation of Lr^{3+} (aq). For methods to determine the single steps, see text.

*This work forms part of a doctoral thesis, Universität Mainz, to be submitted.

**Author to whom correspondence should be addressed.

0020-1693/88/$3.50

logarithm of the distribution coefficients, log K_d, in a given chromatographic system. With a strongly acidic cation-exchange resin as a stationary phase and ammonium α-hydroxyisobutyrate (α-HIB) as a mobile phase, the distribution coefficient and ionic radius can be determined from the elution positions of trivalent Lr and Md relative to the trivalent lanthanides and other trivalent actinides for which the coordination numbers [8] and the ionic radii [8–12] are known. These elements are eluted in the order of their ionic radii, those with the smallest radii (the heaviest lanthanides or actinides) being eluted first [13, 14].

Earlier studies by Silva *et al.* [15] of chemical properties of Lr using the 26-s ^{256}Lr isotope have shown that Lr(III) is the most stable oxidation state in aqueous solution.

Very recently, Hoffman *et al.* [16] performed chemical studies using the 3-min, 8.03 MeV α-activity produced by the ^{249}Bk(^{18}O, α3n) reaction and previously assigned [17] to ^{260}Lr. In these studies, the assignment of this longer-lived 8.03 MeV α-activity to an isotope of element 103 was confirmed. In a preliminary set of manually performed α-HIB elutions from cation-exchange resin columns, Hoffman *et al.* [16] found seven α-events attributable to 3-min ^{260}Lr, with elution positions between the elution positions of Tm^{3+} and Ho^{3+} tracers. The present work with a microprocessor-controlled automated chemistry apparatus was performed in order to confirm this rather unexpected result and to improve its statistical significance. From the distribution coefficients, K_d, we deduced ionic radii and, with the aid of semi-empirical equations, the heats of hydration for Lr^{3+} and Md^{3+}.

Experimental

The 3-min ^{260}Lr isotope and lighter actinides were produced at the Lawrence Berkeley Laboratory 88-inch cyclotron. A target of electro-deposited berkelium oxide on a Be substrate was irradiated with 117 MeV $^{18}O^{5+}$ ions of 5×10^{12} particles per second. The resulting incident energy in the target, after the beam had passed a window foil and the target backing, was 100–101 MeV. Details are given in a companion paper [18]. At the time of the experiments the target consisted of 769 μg/cm^2 ^{249}Bk and 67 μg/cm^2 of its daughter ^{249}Cf. Products from the heavy-ion reaction recoiled into a volume of He gas at 1.3 bar saturated with a KCl aerosol. The He gas and the activity-bearing aerosols were transported by a capillary (i.d. 1.2 mm) to the head of an Automated Rapid Chemistry Apparatus (ARCA) [19]. There the KCl clusters, together with the transported radionuclides, were collected on the surface of a quartz frit through which the transport gas was pumped. In the present experiments, ARCA consisted of two chemically inert HPLC pumps (Latek, Heidelberg) that pumped the various solutions through teflon tubing (i.d. 0.5 mm) to the quartz frit and/or to the columns. Flow rates and times, as well as the operation of the pneumatic slider valves, were controlled by a microcomputer. The collected activity was processed batchwise after 10-min accumulations of the aerosol.

The aerosol, together with the reaction products, was dissolved from the collection frit at room temperature in 300 μl of a 0.05 M α-HIB solution at pH = 4.85 containing the lanthanide tracers (carrier-free ^{171}Tm, ^{171}Er with 9 μg $^{nat.}$Er, and ^{166}Ho with 0.15 μg $^{nat.}$Ho per experiment), added through a sample loop. Compared to the capacity of the columns of about 15 mg, these amounts of carrier are negligible and, in fact, did not change the elution positions of carrier-free lanthanide tracers on pre-calibrated columns. The dissolved reaction products in 0.05 M α-HIB, together with the tracer activities, were pumped to a chromatographic column (2 mm × 60 mm) packed with Aminex A6 cation-exchange resin (particle size 17.5 ± 2 μm) and heated to 80 °C, where the trivalent lanthanides and actinides were strongly adsorbed on the top of the column. These were subsequently eluted from the column with 0.12 M α-HIB at pH = 4.85, pumped at a flow rate of 0.75 ml/min. The pressure built up in the columns was typically 30 bar. Ten fractions of increasing volume from 80 μl to 390 μl were collected consecutively on tantalum disks, that were heated by a hot plate. Evaporation was speeded up by a stream of heated He gas ($T \approx 350$ °C). Lawrencium was eluted between 120 s and 160 s after the end of the collection, and Md between 150 s and 200 s. After flaming, the samples were inserted into the detector array for α-spectroscopy consisting of ten Si(Au)-surface barrier detectors of 300 mm^2 area. The α-events, together with the detector number and the associated time, were recorded and stored in list mode by an on-line data acquisition system. Spontaneous fission events were also recorded. Counting started about 180–240 s after the end of accumulation and lasted for 10 min. Afterwards, all samples were assayed for γ-ray activity with two Ge(Li) diodes in order to determine the distribution of the lanthanide tracer activities.

After the elution was finished, the column was stripped with 0.5 M α-HIB of pH = 4.85 to remove the remaining cations from the resin, which was subsequently regenerated by rinsing with water, 1 M ammonium chloride solution, and 0.05 M α-HIB of pH = 4.85. Then the column was allowed to equilibrate for about 8 min, while, at the same time, another separation was carried out on a second column. With this 'twin-column' set-up we achieved a high repetition rate with a cycle time of 10 min and,

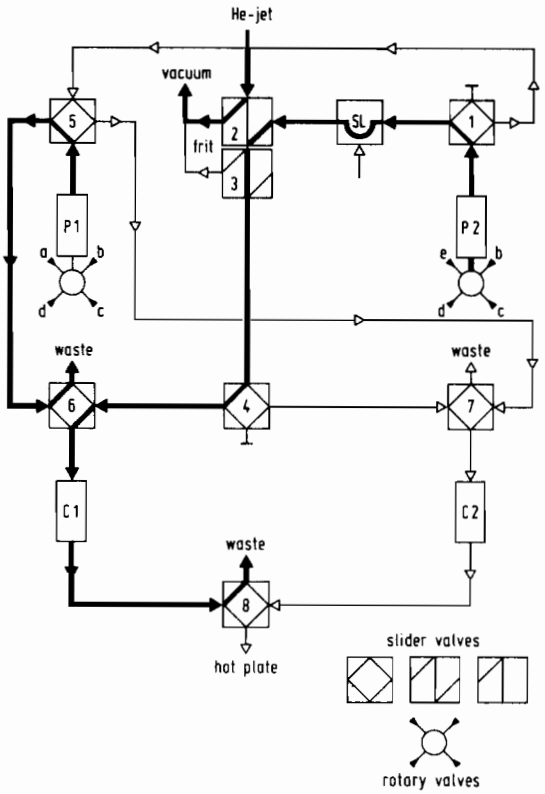

Fig. 2. Schematic configuration of the microprocessor-controlled HPLC system ARCA [19]. The system consists of two pumps (P1 and P2), two cation exchange columns (C1 and C2), which are processed alternately, and pneumatically operated slider valves and rotary valves. Small letters indicate the different stock solutions: (a) 0.12 M α-HIB; (b) 0.5 M α-HIB; (c) 1.0 M NH_4Cl; (d) H_2O; (e) 0.05 M α-HIB.

by using a sufficiently long time for regeneration and equilibration, high reproducibility.

A schematic diagram of the ARCA system as used in the present experiments is shown in Fig. 2. The status of the valves in ARCA during the procedure of dissolving the activity is depicted. The slider valves 2 and 3 have just been switched, so that the jet is directed to the exhaust line and the frit can be washed with 0.05 M α-HIB of pH = 4.85 delivered from pump P2. Lanthanide tracers are added simultaneously by pumping through the previously filled sample loop SL, and loaded together with the reaction products on column C1, while the solution passes through the column and is pumped to the waste through valve 8. Simultaneously, pump P1 rinses the tubing with 0.12 M α-HIB of pH = 4.85 via valves 5 and 6. At the end of the loading procedure, valves 2 and 3 are reset; now the jet deposits the reaction products on top of the frit again. The elution starts by switching valve 6. P1 now pumps 0.12 M α-HIB through column C1 and sample collection begins 1 min later with a switch of valve 8. During that time P2 has pumped 0.05 M α-HIB to C2 as the last step of the regeneration cycle through valves 1, 5 and 7. Then valve 7 is switched to the waste, the rotary valve of P2 is turned and the tubing is rinsed with 0.5 M α-HIB. At the end of the elution, valve 5 is switched disconnecting P1 from C1 and connecting P2 and C1, and valve 8 to the waste. Now C1 is stripped of the remaining cations. The rotary valve at P1 is turned and the tubing rinsed with water. Now P1 and P2 rinse the tubings alternately before the various regeneration procedures of C1 are carried out. Finally, P2 rinses the tubing with 0.05 M α-HIB via valves 1, 5 and 7. At this time, a new processing cycle begins: switching of valves 2 and 3 directs the jet to the exhaust line. P2 pumps through the sample loop, which has been filled manually with tracer solution during the regeneration process, through the frit to valve 4, which is switched to load the activity onto C2 this time. Now the same procedure is performed symmetrically on C2, as described for C1.

Results and Discussion

We performed a total of 93 accumulation and processing cycles, in which we observed the decay of 25 atoms of ^{260}Lr, and about 250 decays of Md isotopes. From the time distribution of the ^{260}Lr decays ($7.90 \leqslant E_\alpha \leqslant 8.10$ MeV) we calculated a half-life of $126 \pm {}^{44}_{18}$ s with a maximum-likelihood method, compatible with the 3 min half-life reported by Eskola *et al.* [17]. As also observed elsewhere [18], this 8 MeV α-group is possibly composed of two peaks, one centered at 7.96 MeV (5 events) and the other at 8.03 MeV (20 events). In Fig. 3.1 the sum of all Lr fractions and in 3.2 the sum spectra of all Md fractions of the corresponding runs are given. In the Lr spectrum one observes only two main activities: ^{260}Lr and ^{211}Bi, a contamination due to a small lead impurity in the target. The Md spectrum shows, besides this contamination, 3.2-h ^{254}Fm (daughter of ^{254}Md), 27-min ^{255}Md and 1.3-h ^{256}Md, as well as 27 spontaneous fission events most likely due to ^{256}Fm, the daughter of ^{256}Md.

From the γ-spectroscopic measurements of all the separated fractions we obtained the volume distribution of lanthanide tracers during the elution process. Due to temporary instabilities in the running conditions of the He jet, varying amounts of KCl were transported to the collection frit, so that the elution positions shifted by a few drops for the different runs. Because of this, each original distribution had to be renormalized by the following procedure, before it was possible to sum up the results from all experiments.

The distribution coefficient K_d between two phases of a chromatographic system is defined as

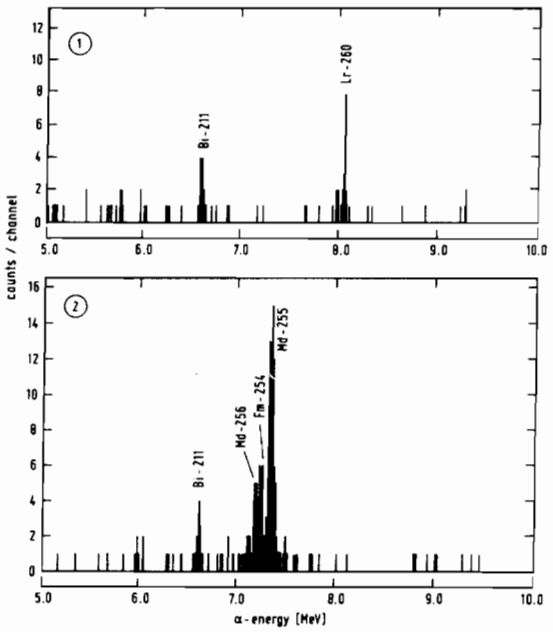

Fig. 3. α-Particle spectra from the elution experiments. Spectrum 3.1 is a sum of all fractions containing ^{260}Lr; spectrum 3.2 a sum of all fractions containing Md activity. A small Pb impurity in the target leads to the contamination by ^{211}Bi. The activities at 6.06 and 8.78 MeV are due to ^{212}Bi which recoiled onto the detectors from a ^{212}Pb (^{212}Bi–^{212}Po) α-energy calibration source.

$$K_d = \frac{V_m - V_f}{V_s} \quad (1)$$

where V_m and V_s are the volumes of the mobile and stationary phases, respectively, and V_f is the free column volume. V_f was determined by passing a solution of ^{137}Cs in 0.1 M α-HIB at pH = 4.85 through the system, V_s from the difference between the geometrical volume of the column and V_f of the column, and V_m from the elution position. For each individual experiment where ^{260}Lr was observed in the α-particle spectra, the values of V_m and their uncertainties were determined from the volume distribution of the three lanthanide tracers by Gaussian fits. The average peak positions for Tm^{3+}, Er^{3+} and Ho^{3+} were found at drop numbers 47, 67 and 100, respectively, in agreement with the relative positions expected from the distribution coefficients compiled by Higgins [20]. These positions were defined as 'ideal', and the centroids of the elution peaks of separations with slightly different elution positions were adjusted to this ideal scale by expanding and compressing the respective drop-number scale. After this normalization step, the peak positions of the lanthanide tracer volume distributions coincided. However, the newly defined volume limits of the ten elution fractions did not coincide any longer. Therefore, the activity per drop was now redistributed into newly defined, coinciding fraction bins of 3 or 5 drops for the lanthanide tracers as well as for the Md and Lr activities, and the redistributed activities of the individual experiments were summed up. The centroids and widths of these summed volume distributions for all activities were independent of the size of the fraction bins. The results for the lanthanide tracers are shown in the upper part of Fig. 4, and for Lr and Md in the lower part. We find that Lr^{3+} elutes together with Er^{3+} and that Md^{3+} elutes close to the Ho^{3+} position. The volumes V_m corresponding to the peak maxima are converted into distribution coefficients by applying eqn. (1). These are listed in Table I together with the reference data for the lanthanides [20].

It is interesting to compare the distribution coefficients of Lr^{3+} and Md^{3+} with their homologous lanthanides Lu^{3+} and Tm^{3+}. This is best done by shifting the logarithmic scales of the K_d values for the lanthanides and actinides such that Md^{3+} is given the same value for the distribution coefficient as Tm^{3+}.

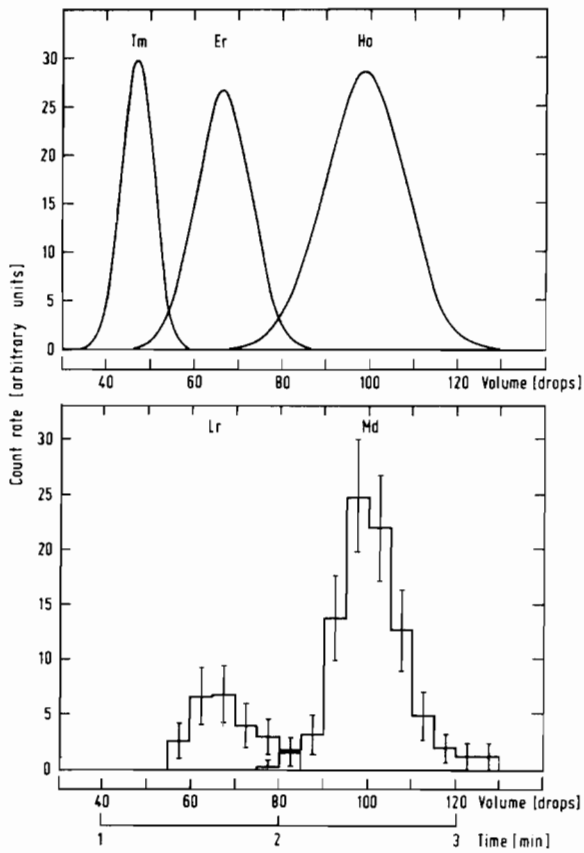

Fig. 4. Sum of the elution curves from the particular runs where ^{260}Lr was detected. The elution of the tracers ^{171}Tm, ^{171}Er and ^{166}Ho are depicted as Gaussian distributions in the upper part; Lr and Md are shown as histograms in the lower part of the figure. Statistical uncertainties (± 1 σ) are indicated. Twenty-five decays of ^{260}Lr and 91 decays of several Md isotopes were observed in this subset of experiments.

TABLE I. Peak Positions and K_d Values for Ln^{3+} Tracers and Lr^{3+} and Md^{3+}

Element	Peak position (drop number)	FWHM	K_d(rel.) [a]
Tm	47.0 ± <0.1	4.4	26.0*
Er	66.7 ± <0.1	7.4	37.0*
Ho	98.6 ± <0.1	10.7	55.0*
Lr	66.7 ± 0.9	8.4	37.0 ± 0.5
Md	100.0 ± 0.2	8.3	56.0 ± 0.1

[a]The K_d values marked by an asterisk are those of Higgins [20]. They are normalized to Cm^{3+} which is arbitrarily set equal to 1000.

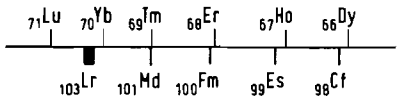

Fig. 5. Distribution coefficients of homologous, trivalent lanthanides and actinides. The two logarithmic scales were arbitrarily adjusted by giving the same value of K_d to Tm^{3+} and Md^{3+}. The experimental value for Lr^{3+} is much closer to Yb^{3+} than to its homologue Lu^{3+}.

The result is shown in Fig. 5. Homologous elements occur at similar positions. Only Lr^{3+} elutes later than one would naively expect: its position is not close to the homologue Lu^{3+}, but close to Yb^{3+} instead.

According to Marcus and Kertes [7], the distribution coefficients reflect the ionic radii. For ions of the same charge and coordination number in a given chemical system $\log K_d$ is a linear function of the ionic radius. From the transport behaviour of lanthanides and some actinides in aqueous solutions it is known that the coordination number (CN) for the heaviest trivalent lanthanides (above Gd) and the heavy actinides (above Cf) is CN = 8 at 25 °C. At higher temperatures the change to CN = 9 for the lighter elements of both series is expected to occur at even lower atomic number [8]. Even though there is no experimental value of CN for Lr^{3+}, it is not expected that this number should deviate from 8. Then, the $\log K_d$ values of the heavier lanthanide and actinide ions, including Lr^{3+}, should constitute a unique, linear relationship to the respective ionic radii.

Traditionally, for elements available in weighable amounts, the basic parameter used in the calculation of thermodynamic quantities is the crystallographic radius. This is obtained from the volume of the unit cell of the crystals These volumes vary linearly with the third power of the radius. For most ionic crystals of trivalent lanthanides the coordination number is CN = 6, and we first used these experimental data (CN = 6) for correlations with the respective ionic radii of the actinides and for the determination of the heats of hydration. The fact that solution chemistry of these ions and their actinide homologues involves hydration number CN = 8 and that the ionic radii vary with CN is of no consequence because the ionic radii to be inserted into the various semi-empirical formulae for the determination of the hydration enthalpy do not have to be known on an absolute scale. This is because the numerical coefficients of these formulae are fixed beforehand by fits to experimentally determined hydration enthalpies. It is also possible to estimate [8] radii with CN = 8, since Shannon [11] gives some ionic radii of lanthanides with several values of CN. Later on, we also used these somewhat larger CN = 8 radii and demonstrated that the heats of hydration resulting from these radii are essentially the same as those obtained before.

There are several sets of crystallographic radii for lanthanide and some actinide ions in the literature [8–12] that are not necessarily compatible. In 1954 Templeton and Dauben [9] published crystallographic radii of trivalent lanthanides with CN = 6, which were confirmed and extended to some trivalent actinides by Haire and Baybarz [10]. A plot of log K_d *versus* these ionic radii is shown in Fig. 6.1. There is an excellent linear correlation, and the correlation seems to be identical for lanthanide and actinide ions, as expected. The distribution coefficients of Md^{3+} and Lr^{3+} can be converted with the slope and intercept of the line to ionic radii, yielding 0.0896 ± 0.0001 nm for Md^{3+} and 0.0881 ± 0.0001 nm for Lr^{3+}. (The use of the mathematical error in the determination of the distribution maxima of Lr and Md would yield 5×10^{-5} nm and 6×10^{-6} nm, respectively. Those errors are orders of magnitudes smaller than the uncertainties of the reference data [9]. Therefore we estimate a more realistic experimental uncertainty of 0.0001 nm.)

Also shown in Fig. 6.1 is the log K_d value for Fm^{3+} as previously determined by Schädel *et al.* [21] in α-HIB elutions performed under very similar conditions. According to our experience, this value is more accurate than the value given by Higgins [20]. This yields, for CN = 6 on the Templeton–Dauben scale, an ionic radius close to 0.0911 nm.

Because, as pointed out by Templeton and Dauben [9], the third decimal of their radii is in doubt on an absolute scale, with the fourth decimal being significant only for the differences of adjacent radii, one should perhaps characterize the present values as follows. The ionic radius of Lr^{3+} is within 0.0001 nm identical to that of Er^{3+}. The difference between the $_{103}Lr^{3+}$ radius and the $_{101}Md^{3+}$ radius is only 0.0015 nm, significantly smaller than the difference of 0.0021 nm for the analogous lanthanide ions, $_{69}Tm^{3+}$ and $_{71}Lu^{3+}$, at the end of the lanthanide series. On the other hand, the difference between the $_{101}Md^{3+}$ radius and the $_{100}Fm^{3+}$ radius (0.0016 nm), as well as the difference between the $_{100}Fm^{3+}$ and the $_{99}Es^{3+}$ radii

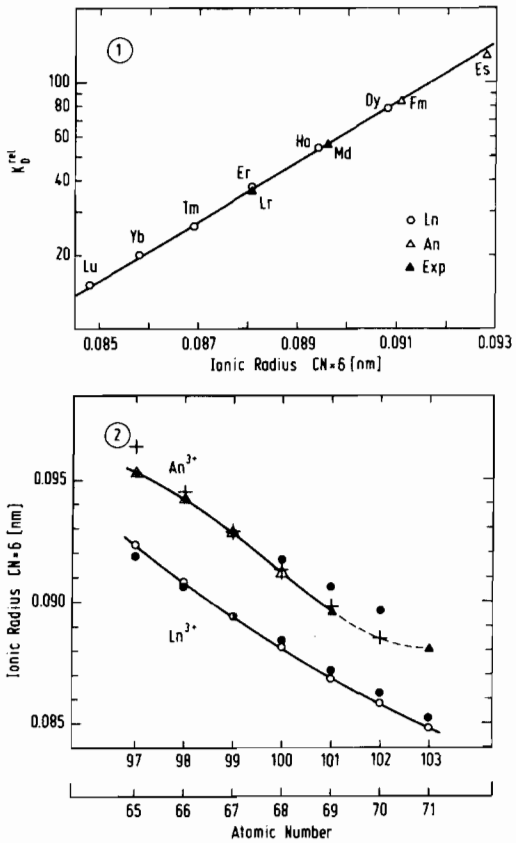

Fig. 6. (1) Relative distribution coefficients K_d [20] plotted logarithmically *vs.* ionic radii for CN = 6 by Templeton and Dauben [9] for some trivalent lanthanide ions (open dots) and for Es^{3+} by Haire and Baybarz [10] (open triangle). This subset of elements is clearly in the linear part of the correlation and not affected by the change of CN which occurs for elements lighter than Gd and Cf, respectively. The solid line is a linear least-squares fit through these reference data. The log K_d for Fm^{3+} (open triangle) is from ref. 21. The data from this work for Md^{3+} and Lr^{3+} are marked by full triangles. (2) Ionic radii for CN = 6 as a function of the atomic number of homologous lanthanides and actinides. The experimental data Ln^{3+} from ref. 9, Bk^{3+}, Cf^{3+} and Es^{3+} from ref. 10, Fm^{3+} from ref. 21, and Md^{3+} and Lr^{3+} (from this work) are indicated by the same symbols as in Fig. 6.1. The lines are to guide the eye. The full points are based on relativistic Dirac–Slater calculations by Waber and Cromer [22], see text. The crosses are based on radial expectation values of the $5f_{7/2}$ orbitals as obtained by the multi-configuration Dirac–Fock method by Desclaux and Freeman [23].

(0.0016 nm), are unusually large compared to the difference of 0.0012 nm for the analogous lanthanide ions. This would indicate that the actinide contraction at the end of the actinide series is more pronounced than the lanthanide contraction, with the exception of the last member of the actinide series where this trend does not continue. In order to complete this experimental information, it appears to be important to measure the ionic radius of No^{3+}. Because nobelium is most stable in aqueous solution in the divalent state, the α-HIB method cannot be used as it will not work under the strongly oxidizing conditions necessary to keep No in the trivalent state. Perhaps extraction chromatography with HDEHP can be adapted to obtain information about the ionic radius of No^{3+} based on its elution position relative to other actinides and lanthanides.

The dependence of the ionic radii and their differences on the atomic number is shown in Fig. 6.2. The crystallographic radii of the lanthanides [9] are compared to calculated radii for Ln^{3+} ions corresponding to the principal maxima in the radial distribution functions of the $5p_{3/2}$ orbitals as obtained by Waber and Cromer [22] in relativistic Dirac–Slater calculations. The latter radii are normalized to the experimental radius of Ho^{3+}. One notes a slight disagreement between the trend of these theoretical radii (full circles in Fig. 6.2) and the trend of the crystallographic radii [9] (open symbols in Fig. 6.2). As for the actinide ions, Waber and Cromer reported values only for U^{3+}, Np^{3+} and Pu^{3+}. These are smaller, by a constant amount, than the respective maxima in the radial distribution functions of the same orbitals ($6p_{3/2}$) in the neutral atoms, the latter being tabulated [22] up to nobelium. If one assumes such a constant shrinking of the radii for the respective ions throughout the actinide series, one obtains estimates of radii for the trivalent actinides, too. These are normalized to the experimental radii at Es^{3+} (see Fig. 6.2). There seems to be a marked deviation at the end of the actinide series of the experimental radii from the estimates based on Dirac–Slater wavefunctions. The heaviest trivalent actinides seem to be systematically too small. Figure 6.2 (crosses) also includes radial expectation values $\langle r \rangle$ of the $5f_{7/2}$ orbitals as obtained in mixed-configuration Dirac–Fock calculations by Desclaux and Freeman [23]. The latter are again normalized to the experimental ionic radii at the Es^{3+} position. Values are given only up to No^{3+} [23]. The much closer agreement of these theoretical values with the trend of the experimental data underlines the importance of a consistent treatment of both relativistic and correlation effects. However, in contrast to their earlier calculations [24], it is the size of the $5f_{7/2}$ orbitals [23] rather than that of the $6p_{3/2}$ orbitals [22, 24] that determines the ionic radii of the heaviest actinides. Unfortunately, no calculated values are given for Lr^{3+} [22, 23] for comparison with our experimental ionic radius. Therefore, we are not able to draw conclusions on the relevance of relativistic effects in determining the ionic radius of Lr^{3+}.

The unusually large ionic radius for Lr^{3+} may possibly be explained in terms of the polarizability of the f-shell electronic orbitals. Since the unfilled

f-orbitals in Er^{3+} ($4f^{11}$), Fm^{3+} ($5f^{11}$), Tm^{3+} ($4f^{12}$) and Md^{3+} ($5f^{12}$) are relatively polarizable, in the determination of the ionic radii the ligands are allowed to be closer to the central 3+ ion. In Lu^{3+} and Lr^{3+}, the filled $4f^{14}$ and $5f^{14}$ shells are relatively less polarizable, forcing the ligands to remain further from the central ion. This would therefore cause a larger apparent ionic radius in both the determinations from crystal structure and from α-HIB elutions. Since the 5f electrons are more extended relative to the 6d in the actinides than the 4f relative to the 5d in the lanthanides, this effect should be more pronounced in the actinides than in the lanthanides, as seems to be indicated by the anomalously large radius of Lr^{3+} measured in this work.

The experimental ionic radii for CN = 6 can now be inserted into semi-empirical equations of Phillips and Williams [4] or of Bratsch and Lagowski [5] to estimate heats of hydration. The first formula yields 3641 ± 1 kJ/mol for Md^{3+} and 3672 ± 1 kJ/mol for Lr^{3+}, the latter 3670 ± 1 kJ/mol and 3703 ± 1 kJ/mol, respectively. As shown in Table II, both these semi-empirical equations, in connection with the radii of Templeton and Dauben [9], are capable of reproducing experimental hydration enthalpies [25] to within 20 kJ/mol. It is reasonable to assume that the hydration enthalpies for Md^{3+} and Lr^{3+} determined in this work are of the same accuracy on an absolute scale.

TABLE II. Heats of Hydration of Lanthanide and Selected Actinide 3+ Ions

Ion	Heat of hydration (kJ/mol)			
	Measured	Calculated		
		1	2	3
La^{3+}	−3320	−3326	−3324	−3377
Ce^{3+}	−3371	−3374	−3373	−3425
Pr^{3+}	−3413	−3412	−3413	−3458
Nd^{3+}	−3442	−3445	−3447	−3489
Pm^{3+}	−3478	−3475	−3478	−3525
Sm^{3+}	−3515	−3504	−3508	−3549
Eu^{3+}	−3548	−3531	−3537	−3580
Gd^{3+}	−3572	−3555	−3561	−3602
Tb^{3+}	−3606	−3585	−3593	−3636
Dy^{3+}	−3637	−3615	−3625	−3666
Ho^{3+}	−3668	−3645	−3655	−3697
Er^{3+}	−3692	−3672	−3684	−3723
Tm^{3+}	−3717	−3697	−3710	−3747
Yb^{3+}	−3740	−3721	−3735	−3769
Lu^{3+}	−3761	−3744	−3758	−3782
Pu^{3+}	−3469	−3460	−3469	−3456
Md^{3+}		−3641	−3670	−3651
Lr^{3+}		−3672	−3703	−3679

Experimental data of lanthanides and plutonium [25] are compared with calculations from ionic radii according to 1. Phillips and Williams [4]; 2. Bratsch and Lagowski [5]; 3. David [8]. The two last lines show the results of calculations based on our experimental ionic radii in the respective models. All data are in kJ/mol at 25 °C, $\Delta H_{hyd}(H^+) = -1114$ kJ/mol.

David *et al.* [6, 8] have criticized the use of such semi-empirical equations because these require, in principle, a separate adjustment of the parameters with experimental data for each series of elements. Even though these parameters are usually constant in a given series, it is claimed by David *et al.* [6, 8] to be unsafe to adopt the lanthanide values for the actinide series. However, this does not appear to be a problem with the one actinide example given in Table II.

Nevertheless, we have made use of the formalism and numerical coefficients proposed by David *et al.* [6] to calculate the hydration enthalpies again. This formalism gives hydration enthalpies consistent with experimental data associated with mono-, di- tri- and tetravalent ions of any series of elements without adjustment of the numerical coefficients. It requires the use of ionic radii corresponding to the true inner-sphere hydration number of the ionic species, and the hydration number itself enters the formula [6].

Thus, we have to discuss the determination of ionic radii for CN = 8, which is the hydration number for the heavy lanthanide ions as well as the heavy actinide ions [8]. The compilation by Shannon [11] is generally believed to be the most consistent set of crystallographic radii for a large number of ions and different coordination numbers. By making use of the linear variation of $r(Ln_z^{2+})$ *versus* $r(Ln_{z+1}^{3+})$ and $r(An_z^{3+})$ *versus* $r(An_{z+1}^{4+})$ for isoelectronic ions with f^n configuration, and by assuming that the difference $r(M_{CN=8}^{3+}) - r(M_{CN=6}^{3+})$ *versus* $r(M_{CN=8}^{3+})$ varies linearly, the set of radii by Shannon [11] was recently modified and completed by David [8]. The use of the numerical coefficients associated with the formula [6] for the determination of the heat of hydration requires the use of David's radii [8].

In Fig. 7.1 we show the correlation of the $\log K_d$ values for trivalent lanthanides with respective ionic radii for CN = 8 [8], which is linear again, as expected. However, when the $\log K_d$ values for Fm^{3+} and Es^{3+} are inserted into the figure with the ionic radii proposed by David [8], one finds that these data points do not fall on the linear correlation of the lanthanide data, but seem to suggest a separate correlation, possibly having the same slope. If one assumes the same slope, our experimental values of $\log K_d$ for Md^{3+} and Lr^{3+} would define ionic radii of 0.1028 ± 0.0001 nm and 0.1016 ± 0.0001 nm, respectively. The value for Md^{3+} is exactly the same as predicted by David [8]; the value for Lr^{3+} is 0.0016 nm larger than predicted [8]. Thus, again, one is led to conclude that the difference between the Md^{3+} and the Lr^{3+} radii, 0.0012 nm, is unusually small for a step of two in the atomic number. Finally, the heats of

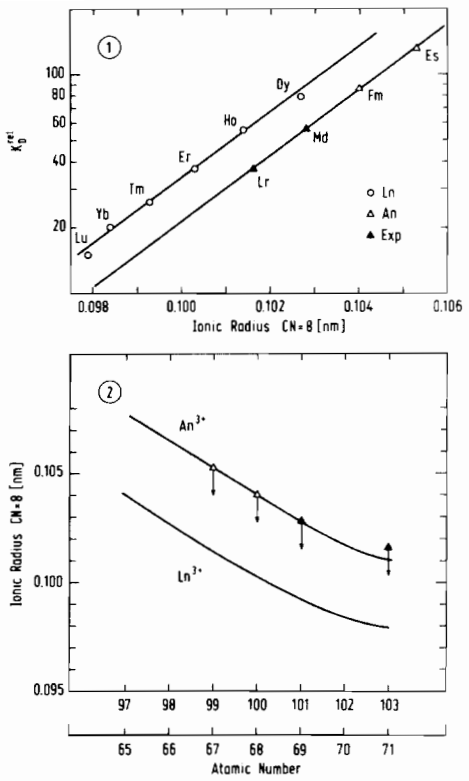

Fig. 7. (1) Same as Fig. 6.1, except that the ionic radii for CN = 8 are those of David [8] which are based on the compilation by Shannon [11]. The solid line is a linear least-squares fit through the lanthanide data. The line through the actinide data has the same slope and is fixed at the Es^{3+} value. Surprisingly, the lines are shifted against each other by 0.0012 nm. This is inconsistent with experimental data which give no justification to assume different correlations for lanthanides and actinides above Gd and Cf. (2) Ionic radii for CN = 8 for homologous lanthanides and actinides as given by David [8] (solid lines). Experimental actinide data corresponding to the actinide correlation in Fig. 7.1 are indicated by the same symbols as in Fig. 6. The arrows mark the ionic radii which result from taking the same correlation for lanthanides and actinides.

hydration results as 3651 ± 1 kJ/mol for Md^{3+} and 3679 ± 1 kJ/mol for Lr^{3+}, see Table II, which agree to within 20 kJ/mol with the results obtained with the semi-empirical equations by Phillips and Williams [4] and by Bratsch and Lagowski [5] and the radii of ref. 9. It is gratifying to see that, through adjustment of the respective numerical coefficients, the uncertainties in the absolute size of the ionic radii do not enter into the determination of the thermodynamic quantity of interest, the enthalpy of hydration.

Still, the two separate lines in Fig. 7.1 await an explanation. A change in the coordination number is ruled out experimentally [8]. (In both series, there is a change to CN = 9 towards the lighter elements, occurring for the actinides around Bk^{3+} at 25 °C. For higher temperatures this change of the coordination number is expected at still lower atomic number for the respective series.) There is no reason to believe that the type of chemical interaction between a Ln^{3+} ion and the cation exchanger is different than for an An^{3+} ion. Then, according to Marcus and Kertes [7], the ionic radius is the only parameter to be considered. The two separate lines for lanthanides and actinides (Fig. 7.1) would then indicate that David's two sets of radii for trivalent lanthanide and actinide ions are incompatible with each other. We are convinced that this is actually the case. According to David's tables, Cf^{3+} has the same ionic radius as Eu^{3+} both for CN = 6 and for CN = 8. Thus the two elements should elute at the same position. However, it is well established that Cf^{3+} elutes with Gd^{3+}. The same observation is made for the heavier Ln^{3+} and An^{3+} ions. The tables of ref. 8 predict elution of Es^{3+} with Gd^{3+}, Fm^{3+} with Tb^{3+}, Md^{3+} with Dy^{3+}, and Lr^{3+} close to Ho^{3+}. However, the experiment shows correlations between Es^{3+} and Tb^{3+}, Fm^{3+} and Dy^{3+}, Md^{3+} and Ho^{3+}, and Lr^{3+} and Er^{3+}; for the latter two, see Fig. 4. The situation is illustrated in Fig. 7.2, where we show the radii of ref. 8 and the experimental radii obtained from the (separate) correlation of $\log K_d$ with the ionic radius for trivalent actinides from Fig. 7.1 (triangles). In order to make the An^{3+} radii compatible with the Ln^{3+} radii according to their elution positions, one would have to make all An^{3+} radii smaller by 0.0012 nm. These smaller actinide radii are also indicated in Fig. 7.2 by arrows.

Conclusions

We have determined the elution positions of Lr^{3+} and Md^{3+} ions from a strongly acidic cation-exchange resin in buffered ammonium α-hydroxyisobutyrate solution at pH = 4.85 relative to the trivalent lanthanide ions Tm^{3+}, Er^{3+} and Ho^{3+}. We find that Lr^{3+} elutes with Er^{3+} and Md^{3+} elutes close to the Ho^{3+} position. For the trivalent lanthanide ions the $\log K_d$ values resulting from the elution positions correlate linearly with the crystallographic radii for CN = 6 by Templeton and Dauben [9]. Also the $\log K_d$ values for Es^{3+} and the Es^{3+} crystallographic radius reported by Haire and Baybarz [10] fall in line with this linear correlation. Based on this correlation, the $\log K_d$ values for Fm^{3+}, Md^{3+} and Lr^{3+} indicate that the ionic radius of Fm^{3+} is 0.0016 nm smaller than that of Es^{3+}, the ionic radius of Md^{3+} is 0.0016 nm smaller than that of Fm^{3+}, and the ionic radius of Lr^{3+} is 0.0015 nm smaller than that of Md^{3+}, even though there is a $2Z$ separation. These differences indicate that the actinide contraction towards the end of the actinide series is stronger than the lanthanide contraction, with a relative increase in the difference $D = r(An^{3+}) - r(Ln^{3+})$ for the last members of both

series, Lu^{3+} and Lr^{3+}. The set of radii by Templeton and Dauben [9] is found to be in fair agreement with ionic radii deduced from relativistic Dirac–Slater wave functions by Waber and Cromer [22], with maximum deviations of ±0.0005 nm between Tb^{3+} and Lu^{3+}. A comparison of the actinide ionic radii with estimates based on the same relativistic calculations indicates good agreement for Bk^{3+}, Cf^{3+} and Es^{3+}, while the experimental ionic radii of Fm^{3+}, Md^{3+} and Lr^{3+} are smaller than the estimates by 0.0004 nm, 0.0010 nm, and ~0.0005 nm, respectively. More recent relativistic calculations [23] using multi-configuration wave functions are in better agreement with the trend of the experimental radii. This demonstrates the importance of a consistent treatment of both relativistic effects and configuration mixing.

If the $\log K_d$ values are correlated to the set of ionic radii proposed by David [8], it is found that trivalent lanthanides and actinides constitute two separate correlations. It is concluded that there is an internal inconsistency between David's lanthanide and actinide ionic radii. One possible way to remove this discrepancy is to make the radii of the heaviest actinides smaller by 0.0012 nm relative to their lanthanide homologues. It is then again indicated by the data that the relative distance $D = r(An^{3+}) - r(Ln^{3+})$ is smallest for the Md^{3+}–Tm^{3+} pair.

Fortunately, these open questions concerning the absolute scale of the ionic radii are of no consequence for the deduction of the enthalpies of hydration. This is because the respective semi-empirical formulae [4–6] use numerical coefficients adjusted in each case to a particular set of ionic radii in order to obtain maximum consistency with experimental hydration enthalpies. The heats of hydration resulting from the three different concepts for Md^{3+} and Lr^{3+} agree within 30 kJ/mol. Their arithmetic mean is 3654 ± 12 kJ/mol for Md^{3+} and 3685 ± 13 kJ/mol for Lr^{3+}. Thus, the systematic uncertainties seem to be well within the required [3] margin of 20 kJ/mol (0.2 eV).

Acknowledgements

The authors are grateful to E. Jäger, B. Schausten and S. Zauner for their invaluable help during the preparation of the experiments. Four of us (W.B., M.S., J.V.K. and U.W.S.) have enjoyed the hospitality of the Lawrence Berkeley Laboratory Nuclear Science Division. We would like to thank the staff and crew of the 88-inch cyclotron at LBL for providing stable beams of ^{18}O and technical support. We are indebted to R. W. Lougheed for providing the ^{171}Tm tracer, and to H. Nitsche for the loan of some laboratory equipment. We are grateful to F. David for comments and suggestions concerning ionic radii and semi-empirical models for the calculation of heats of hydration.

We are indebted for the use of the target material to the Office of Basic Energy Sciences, U.S. Department of Energy, through the transplutonium element production facilities at the Oak Ridge National Laboratory.

H.L.H. was supported by a National Science Foundation Graduate Fellowship.

This work was supported by the German Federal Minister for Research and Technology (BMFT) under Contract No. 03 HE1MAI. This work was supported in part by the Director, Office of the Energy Research, Division of Nuclear Physics of the Office of High Energy and Nuclear Physics of the U.S. Department of Energy under Contract No. DE-AC03-76SF00098.

References

1 L. J. Brewer, *J. Opt. Soc. Am., 61,* 1101 (1971).
2 J.-P. Desclaux and B. Fricke, *J. Phys., 41,* 943 (1980).
3 O. L. Keller, *Radiochim. Acta, 37,* 169 (1984).
4 C. S. G. Phillips and R. J. P. Williams, 'Inorganic Chemistry', Vol. 2, Oxford University Press, London, 1966, p. 58.
5 S. G. Bratsch and J. J. Lagowski, *J. Phys. Chem., 90,* 307 (1986).
6 F. David, B. Fourest and J. Duplessis, *J. Nucl. Mater., 130,* 273 (1985).
7 Y. Marcus and A. S. Kertes, 'Ion Exchange and Solvent Extraction of Metal Complexes', Wiley-Interscience, New York, 1969, p. 287.
8 F. David, *J. Less-Common Met., 121,* 27 (1986); F. David, *J. Chim. Phys., 83,* 393 (1986).
9 D. H. Templeton and C. H. Dauben, *J. Am. Chem. Soc., 76,* 5237 (1954).
10 R. G. Haire and R. D. Baybarz, *J. Inorg. Nucl. Chem., 35,* 489 (1973).
11 R. D. Shannon, *Acta Crystallogr., Sect. A, 32,* 751 (1976).
12 S. Goldmann and L. Morss, *Can. J. Chem., 53,* 2695 (1975).
13 G. R. Choppin, B. G. Harvey and S. G. Thompson, *J. Inorg. Nucl. Chem., 2,* 66 (1955).
14 H. L. Smith and D. C. Hoffman, *J. Inorg. Nucl. Chem., 3,* 243 (1956).
15 R. J. Silva, T. Sikkeland, M. Nurmia and A. Ghiorso, *Inorg. Nucl. Chem. Lett., 6,* 733 (1970).
16 D. C. Hoffman, R. A. Henderson, K. E. Gregorich, D. A. Bennett, R. M. Chasteler, C. M. Gannett, H. L. Hall, D. M. Lee, M. J. Nurmia, S. Cai, R. Agarwal, A. W. Charlop and Y. Y. Chu, 'Proc. Conf. on Methods and Applications of Radioanalytical Chemistry, Kona, Hawaii, April 1987', *J. Radioanal. Chem.,* to be published.
17 K. Eskola, P. Eskola, M. Nurmia and A. Ghiorso, *Phys. Rev., C4,* 632 (1971).
18 U. W. Scherer, J. V. Kratz, M. Schädel, W. Brüchle, K. E. Gregorich, R. A. Henderson, D. Lee, M. Nurmia and D. C. Hoffman, *Inorg. Chim. Acta, 146,* 249 (1988).
19 M. Schädel, W. Brüchle and B. Haefner, *Nucl. Instrum. Methods, A264,* 308 (1988).
20 G. H. Higgins, 'The Radiochemistry of the Transcurium Elements', U.S. National Academy of Science, Nuclear Science Series, NAS-NS-3031, 1960.

21 M. Schädel, W. Brüchle, M. Brügger, H. Gäggeler, K. J. Moody, K. Sümmerer, E. K. Hulet, A. D. Dougan, R. J. Dougan, J. H. Landrum, R. W. Lougheed, J. F. Wild and G. D. O'Kelley, *Phys. Rev., C33,* 1547 (1986); personal communication.
22 J. T. Waber and D. T. Cromer, *J. Chem. Phys., 42,* 4116 (1965).
23 J.-P. Desclaux and A. J. Freeman, Atomic properties of the actinides, in A. J. Freeman and G. H. Lander (eds.), 'Handbook on the Physics and Chemistry of the Actinides', North-Holland, Amsterdam, 1984, p. 1.
24 J.-P. Desclaux, *At. Data Nucl. Data Tables, 12,* 311 (1973).
25 L. R. Morss, *J. Phys. Chem., 75,* 392 (1971).